Charge-transfer rates for xenon Rydberg atoms at a metal surface

S. Wethekam,[1] H. R. Dunham,[2] J. C. Lancaster,[2] and F. B. Dunning[2]
[1]*Institut für Physik der Humboldt-Universität zu Berlin, Newtonstr. 15, D-12489 Berlin, Germany*
[2]*Department of Physics and Astronomy and the Rice Quantum Institute, Rice University, MS-61, 6100 Main Street, Houston, Texas 77005-1892, USA*
(Received 8 December 2005; published 9 March 2006)

The ionization of xenon Rydberg atoms excited to the lowest states in the $n=17$ and $n=20$ Stark manifolds at a flat Au(111) surface is investigated. Despite the strong perturbations in the energies and structure of the atomic states that occur as the surface is approached, it is shown that, under appropriate conditions, each incident atom can be detected as an ion and that the experimental data can be well fit by assuming that the ionization rate on average increases exponentially as the surface is approached. The ionization rates are compared to theoretical predictions.

DOI: 10.1103/PhysRevA.73.032903 PACS number(s): 34.50.Dy, 79.20.Rf

Charge exchange between atoms and surfaces is important in many practical applications ranging from the catalytic processes that occur in fuel cells to the operation of nanoscale electronic devices. Rydberg atoms in which one electron is excited to a state of large principal quantum number n provide a particularly sensitive probe of such charge exchange. Because of their large physical size and weak binding Rydberg atoms are strongly perturbed by the presence of a nearby metal surface. Even relatively far from the surface, the motion of the excited electron can be strongly influenced by image charge interactions that distort the electronic wave functions and shift the atomic energy levels. Furthermore, ionization can occur through resonant tunneling of the excited electron into a vacant level in the metal which causes the states to become very broad even relatively far from the surface. Theoretical treatments of the problem are facilitated because at such distances the Rydberg electron-surface interaction can be modeled by classical image interactions and structural details of the surface, such as lateral corrugations, are unimportant.

Initial theoretical studies focused on hydrogen Rydberg atoms, first using perturbation methods [1]. More recently, the complex scaling and time-dependent close-coupling techniques have been used as well as the etalon equation method [2–6]. These calculations provided insights into the changes in the spatial characteristics of the states that occur as the surface is approached. Hybridized "Stark-like" states are formed, the electron probability density for some of which are maximal towards the surface, others towards vacuum. The tunneling rates, which depend critically on the overlap between the electronic wave function and the surface, were predicted to vary widely from state to state and to be many orders of magnitude greater for states oriented toward the surface. More recently, to permit direct comparison to experimental measurements, calculations for xenon Rydberg atoms have been undertaken [7–10]. These show that the energy-level shifts associated with the perturbations introduced by the surface can lead to crossings between neighboring levels as the surface is approached. If these crossings are traversed adiabatically and the states involved have very different spatial characteristics, this can lead to dramatic changes in the tunneling rate as the atom successively assumes the character of states oriented towards and away from the surface and loses much of its initial identity.

Experimental estimates of the atom-surface separation at which ionization occurs, i.e., the ionization distance, were obtained using alkali Rydberg atoms by measuring their transmission through micrometer-sized slits or by observing directly the ion signal resulting from their surface ionization [11–13]. Detailed interpretation of the data, however, was problematic because alkali deposition can lead to the production of localized electric fields at a surface [14]. More recently these problems have been circumvented by the use of xenon Rydberg atoms which do not stick to, or react chemically with, a target surface permitting measurements under stable well-defined conditions [10,15]. In initial studies, the threshold distances at which ionization occurred were determined and found to be in reasonable accord with hydrogenic theory. Subsequent experiments using Rydberg atoms initially prepared in states oriented towards and away from the surface showed that such states ionize at similar atom-surface separations, consistent with the curve crossing picture [7–10]. In the present work we extend these earlier measurements by obtaining absolute surface ionization efficiencies taking into account the radiative decay of Rydberg atoms as they approach the surface. Model fits to the data are used to estimate the electron tunneling rates and their dependence on atom-surface separation, and these are compared to theoretical predictions.

The present apparatus is shown in Fig. 1 and is described in detail elsewhere [15,16]. Briefly, xenon Rydberg atoms are directed at near grazing incidence onto a Au(111) target surface. Ions formed by tunneling are attracted to the surface by the electric field associated with their image charges. These fields are large and will rapidly accelerate an ion to the surface where it will be neutralized by an Auger process. To prevent this, an ion collection field is applied perpendicular to the surface. Because the initial image-charge field experienced by an ion, and thus the external field required to counteract it, depends on the atom-surface separation Z at which ionization occurs, ionization distances can be inferred from measurements of the surface ionization signal as a function of the ion collection field.

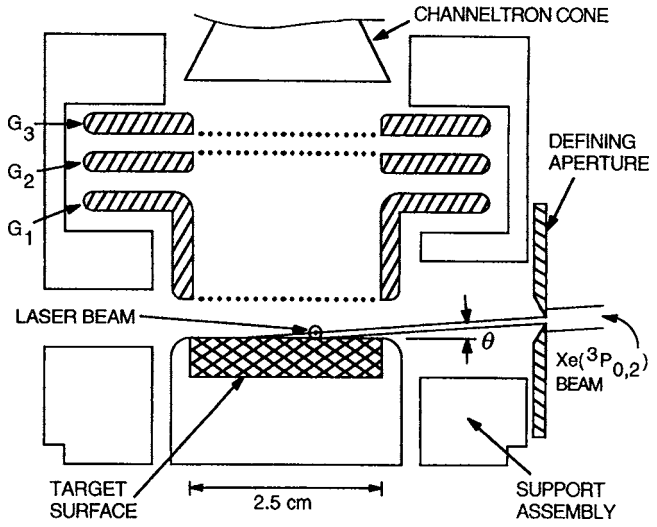

FIG. 1. Schematic diagram of the apparatus.

Xenon Rydberg atoms are created by photoexciting $^3P_0$ atoms contained in a mixed Xe($^3P_{0,2}$) metastable atom beam that is produced by electron impact excitation of ground-state atoms contained in a supersonic expansion. The beam is tightly collimated by an 80-μm-wide aperture before striking the target surface to obtain a well defined grazing angle of incidence $\theta \sim 4°$. The atoms are excited close to the surface using the crossed output of an extracavity-doubled CR899-21 Ti:sapphire laser that is polarized perpendicular to the surface to selectively populate $m=0$ states. Experiments are conducted in a pulsed mode by forming the output of the (cw) laser into a train of pulses of ~ 1 μs duration and ~ 5 kHz repetition frequency using an acousto-optic modulator. Excitation occurs in a weak dc field to allow creation of selected (oriented) Stark states. Here the lowest members of the $n=17$ and $n=20$ Stark manifolds, which correlate with the zero-field $17f$ and $20f$ states and are initially strongly oriented towards the surface, are excited. Immediately following each laser pulse, a strong pulsed ion collection field of ~ 1 μs risetime and ~ 20 μs duration is applied. Ions that escape the surface are accelerated to a bell-mouthed channeltron for detection. (The probability that a Rydberg atom is created by any laser pulse is small, <0.1, and data must be accumulated following many laser pulses.) Because the Rydberg-atom flight times to the surface from their point of creation is typically ~ 5 μs, time-of-flight techniques coupled with arrival time gating can be used to discriminate those ions produced in atom-surface interactions from those produced by laser-induced photoionization or, if the ion collection field is sufficiently large, by direct field ionization. If tunneling occurs at an atom-surface separation Z_i, the minimum external field (in a.u.) that must be applied to prevent the ion striking the surface and being lost is

$$E_{\min}(Z_i, T_\perp) = \left[\frac{1}{2Z_i} + \sqrt{\frac{T_\perp}{Z_i}} \right]^2, \qquad (1)$$

where $T_\perp \equiv m v_\perp^2 / 2$ is the kinetic energy of the atom perpendicular to the surface at the time of ionization. Thus by measuring the surface ionization signal as a function of ion collection field the range of ionization distances can be deduced.

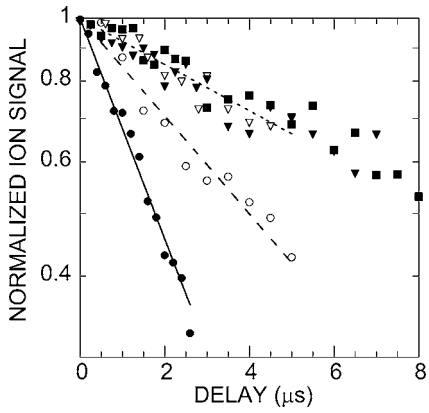

FIG. 2. Time evolution of the population of Xe ($n=17$) atoms in fields of: ●, 0 V cm^{-1}; ○, 200 V cm^{-1}; ■, 1 kV cm^{-1}; ▽, 2 kV cm^{-1}; and ▼, 3 kV cm^{-1}. Each data set is normalized to the number of Rydberg atoms initially created. The lines correspond to lifetimes of: (——) 2.5 μs; (– – –) 5.6 μs; and (- - - -) 13 μs.

To obtain the absolute efficiency with which Rydberg atoms striking the surface are detected as ions the number of Rydberg atoms incident on the surface must be determined. This is governed by the number initially created by the laser and the number lost through radiative decay during travel to the surface. To measure the Rydberg atom production rate a large pulsed electric field sufficient to field ionize the atoms is applied immediately following excitation and the number of resulting ions is observed. The lifetime of the Rydberg atoms is obtained by monitoring the decrease in this signal as the time delay between excitation and application of the ionizing field is increased. (To extend the time period over which measurements could be undertaken without loss due to collisions with the surface, the point at which Rydberg-atom excitation occurred was moved far from the surface.) The Rydberg-atom lifetime is strongly influenced by the presence of the ion collection field. This is illustrated for $n=17$ in Fig. 2 which shows the time evolution of the Rydberg population for several different applied fields. In zero field the lifetime is relatively short, ~ 2.5 μs, consistent with earlier measurements [17]. Application of even a modest electric field, however, results in a marked increase in lifetime which for fields above ~ 1 kV cm^{-1} becomes quite long, ~ 13 μs. Similar behavior is also seen for $n=20$, the lifetime increasing to >20 μs at fields >500 V cm^{-1}. The velocity distribution of the incident atoms was determined by exciting the Rydberg atoms a known distance from the surface and observing the time dependence of the surface ion signal using a large ion-collection field. (The atom flight times to the surface were kept relatively short (~ 5 μs) to reduce losses associated with radiative decay.) The measured velocity distribution is shown in the inset in Fig. 3 and peaks at a velocity of $\sim 4 \times 10^4$ cm s^{-1}.

Figure 3 shows the applied-field dependence of the surface ion signal observed when xenon $n=17$ and $n=20$ Rydberg atoms are incident on the flat Au(111) target surface. The ion signal is normalized to the number of Rydberg atoms

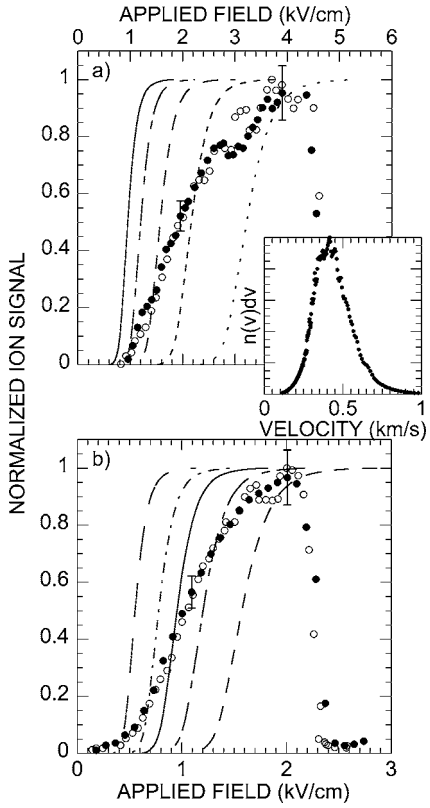

FIG. 3. Applied field dependence of the surface ion signals measured for (a) Xe ($n=17$) and (b) Xe ($n=20$) atoms. The present measurements (●) are normalized to the number of atoms that strike the target surface (see text). Results of earlier measurements (○) [10] are included and are normalized to the present data. The solid lines show the results of model calculations undertaken assuming that ionization occurs at atom-surface separations Z_s of: (····) 800 a.u.; (- - -) 1000 a.u.; (— —) 1200 a.u.; (— - — -) 1400 a.u.; (——) 1600 a.u.; (– – – -) 1800 a.u.; and (— —) 2200 a.u. (see text). The velocity distribution of the incident atoms is shown in the inset.

that initially impact the surface. The error bars indicate the experimental uncertainty. This results from both statistical error and from a number of small systematic effects that are associated with scanning the (pulsed) ion collection field. This leads to changes in the residual field present in the experimental volume at the time of photoexcitation which can change the photoexcitation rate. Also included in Fig. 3 are the results of earlier measurements [10] that have been normalized to the present data. The data show that each incident atom undergoes surface ionization forming an ion that can, with sufficiently large collection fields, be detected with essentially unit efficiency. The sudden decrease in surface ion signal evident at large applied fields is due to direct field ionization of the Rydberg atoms in vacuum before they reach the surface.

The critical threshold fields E_c at which surface ionization signals are first detected are similar to those seen in earlier studies [10,15]. As discussed previously, these correspond to ionization distances of $\sim 4.5\, n^2$ a.u. In the present work, rather than simply considering the threshold fields, the entire surface ionization profile is modeled to examine how the ionization rate varies with atom-surface separation.

The probability that an incident ion will ionize at atom-surface separations in the range $Z \rightarrow Z - dZ$, i.e., in the corresponding time interval $t \rightarrow t + dt$, is given by

$$dP = -P(Z,E,\nu_\perp)\Gamma(Z,E)dt = -P(Z,E,\nu_\perp)\Gamma(Z,E)\frac{dZ}{|\nu_\perp|}, \tag{2}$$

where $P(Z,E,\nu_\perp)$ is the probability for an incident atom to survive passage to a distance Z from the surface and $\Gamma(Z,E)$ is tunneling rate, i.e., the width of the state, at this point. Integration yields

$$P(Z,E,\nu_\perp) = \exp\left\{-\int_Z^\infty \frac{\Gamma(Z',E)}{|\nu_\perp|}dZ'\right\}. \tag{3}$$

(As will be discussed, the width of the state, and thus the survival probability, is influenced by the presence of the ion collection field E.) The fraction of incident atoms with some initial perpendicular velocity $\nu_\perp$ that undergo ionization before approaching within some critical distance Z_{crit} is given by $1-P(Z_{crit},E,\nu_\perp)$. Taking into account the distribution $f(\nu_\perp)$ of atomic velocities perpendicular to the surface, which can be obtained from the Rydberg-atom velocity distribution, the fraction of incident Rydberg atoms that will be detected as ions using an ion collection field E may then be written

$$F(E) = \int_0^\infty f(\nu_\perp)\{1 - P(Z_{crit},E,\nu_\perp)\}d\nu_\perp, \tag{4}$$

where Z_{crit} is related to E and $\nu_\perp$ by Eq. (1), i.e.,

$$Z_{crit} = \frac{T_\perp}{4E}\left\{1 + \sqrt{1 + \frac{2\sqrt{E}}{T_\perp}}\right\}^2. \tag{5}$$

Substitution for $P(Z_{crit},E,\nu_\perp)$ in Eq. (4) yields

$$F(E) = 1 - \int_0^\infty f(\nu_\perp)\exp\left\{-\int_{Z_{crit}(E,\nu_\perp)}^\infty \frac{\Gamma(Z',E)}{|\nu_\perp|}dZ'\right\}d\nu_\perp. \tag{6}$$

To test the role that the velocity distribution $f(\nu_\perp)$ plays on the buildup of the surface ion signal, calculations were undertaken assuming that the ionization rate $\Gamma(Z',E)$ can be represented by a "steplike" function

$$\Gamma(Z',E) = 0 \quad Z' > Z_s$$
$$= \infty \quad Z' \leqslant Z_s, \tag{7}$$

i.e., assuming that ionization occurs at a specific fixed distance Z_s from the surface. The results of calculations employing such a form for $\Gamma(Z',E)$ are presented in Fig. 3 for several values of Z_s. Although the distribution in $\nu_\perp$ broadens the onset in the surface ionization signal it is clear that this distribution by itself cannot account for the experimental observations and that ionization must occur over a range of atom-surface separations. (As Rydberg atoms approach the surface they experience an attractive force due to the dipole-

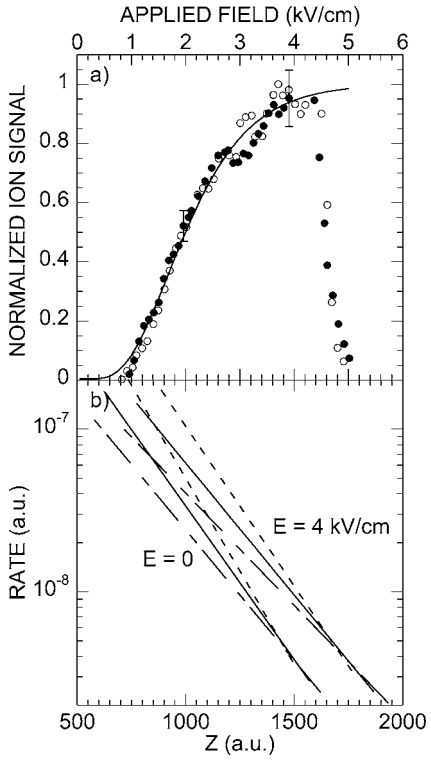

FIG. 4. (a) ——, optimized fit to the experimental data for (a) Xe ($n=17$) atoms assuming an ionization rate of the form in Eq. (8). (b) ——, ionization rates determined from the fit as a function of atom-surface separation for the applied fields indicated. The dashed lines indicate the uncertainties in these rates (see text).

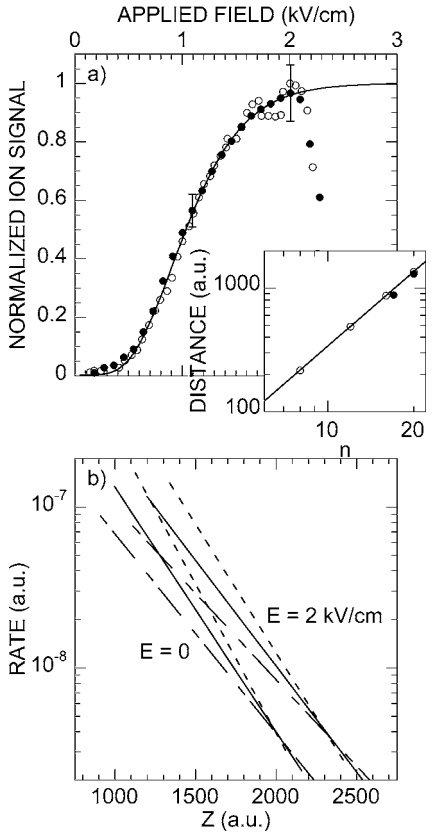

FIG. 5. (a) ——, optimized fit to the experimental data for Xe ($n=20$) atoms assuming an ionization rate of the form Eq. (8). (b) ——, ionization rates determined from the fit as a function of atom-surface separation for the applied fields indicated. The dashed lines indicate the uncertainties in these rates (see text). The inset shows the most probable ionization distances measured in this work (●) and calculated using hydrogenic theory (○) (Ref. [6]) as a function of n. The solid line indicates $3.4n^2$ scaling.

induced dipole interaction. Calculations, however, show that this leads to only small increases in $\nu_\perp$ prior to ionization that are not important for the present analysis.)

The experimental data are fit by assuming that, on average, the ionization rate simply increases exponentially as the surface is approached and can be written as

$$\Gamma(Z',E) = \Gamma_0 \exp\left\{-\frac{Z'(1-kE_0)}{Z_{\text{decay}}}\right\}, \tag{8}$$

where $E_0 \equiv n^4 E$ is the ion collection field classically scaled to the principal quantum number of the incident atoms and Γ_0, Z_{decay}, and k are constants. Use of such an expression is suggested by hydrogenic theory which indicates that the widths of many hydrogenic states initially increase exponentially as the atom-surface separation decreases. The situation for xenon is more complex, because for $n=17$ and $n=20$, the critical threshold ion collection fields E_c are greater than the fields at which states in neighboring Stark manifolds first cross. In this regime the strong perturbations in the energies and structure of the atomic states induced by the presence of the surface lead to a series of avoided crossings as the surface is approached [10]. If these are traversed adiabatically the width of a particular initial state will undergo dramatic changes as the atom successively assumes the character of states oriented towards and away from the surface. However, given a sizable number of such crossings it is not unreasonable to approximate the ionization rate by some more slowly varying overall average. (If the avoided crossings are traversed partially adiabatically and partially diabatically different incident atoms will evolve along different paths but atoms following each path will again transition between states oriented towards and away from the surface.)

The factor $(1-kE_0)$ included in Eq. (8) recognizes that the presence of the ion collection field increases the ionization rate at a given atom-surface separation Z (by lowering the potential barrier between the atom and surface) or, equivalently, that a particular ionization rate is obtained further from the surface. The value of k is derived from earlier calculations of the field dependence of the ionization rates for selected $n=10$ and $n=13$ hydrogenic states [3,15]. These point to a near linear increase with field in the separation at which a given ionization rate is achieved and show that, when the field is expressed in scaled units, k is approximately constant and given by $k=4.2\times10^{-7}$ cm kV^{-1}. Fits to the experimental data obtained using this value of k and the expression for Γ in Eq. (8) are presented in Figs. 4(a) and 5(a). The corresponding ionization rates are shown in Figs. 4(b) and 5(b) as a function of atom-surface separation for representative values of the applied field. The dashed lines provide a measure of the uncertainties in the calculated rates.

These were estimated by assuming systematic errors of +10% and −10% in the measured normalized ion signals (equal to the anticipated experimental uncertainty) and fitting the resultant data sets.

It is interesting to compare the inferred ionization rates with theoretical predictions. The characteristic decay lengths Z_{decay} obtained from the fits, ~230 a.u. for $n=17$ and ~285 a.u. for $n=20$, are much larger than those suggested by the etalon equation method which for the extreme $H(n=20)$ $m=0$, $n_1=0$ Stark state amount to ~25–30 a.u. [6]. Such decay lengths would result in very rapid onsets in the ionization signal similar to those shown in Fig. 3 for ionization at fixed atom-surface separations Z_s. This discrepancy between hydrogenic theory and experiment cannot be attributed to experimental artifacts. While the presence of stray fields at the surface could lead to a broadening of the onset, such fields are believed to be unimportant because the data have been reproduced using different surfaces and because the broadening for $n=20$ sets an upper limit on the size of such fields of $\sim\pm 400$ V cm^{-1}, which is much too small to account for the broadening seen at $n=17$ (and $n=15$ [10]). Furthermore, the discrepancy cannot be associated with the choice of k in Eq. (8) as tests show that the values of Z_{decay} derived from fitting the data are insensitive to the exact value of k. The differences therefore must be attributed to the complex evolution of xenon Rydberg atoms as the surface is approached. Earlier calculations [7–10] have shown that avoided crossings lead to dramatic variations in the width of individual states, which no longer simply increase monotonically with decreasing atom-surface separation. Detailed calculations [10] of these variations have been undertaken for adiabatic evolution of the zero-field Xe($15f$) state. If these are "averaged" by an exponential the resulting decay length, $Z_{\mathrm{decay}}\sim 100$ a.u., is in better accord with the present measured values.

Given the avoided crossings that occur as a xenon Rydberg atom approaches the surface, it is reasonable to expect that the atom-surface separations at which ionization is most probable, i.e., where $d^2P/dZ^2=0$, might be comparable to those for the more strongly surface oriented hydrogenic states because, sufficiently close to the surface, once an atom assumes the character of such a state ionization will be rapid. In zero applied field, the most probable ionization distance is given by

$$Z=-Z_{\mathrm{decay}}\ln\frac{|\nu_\perp|}{Z_{\mathrm{decay}}\Gamma_0}. \tag{9}$$

For $n=17$ and $n=20$ these distances are ~875 and ~1300 a.u., respectively, assuming $\nu_\perp\sim 29$ ms^{-1}. These are plotted in the inset in Fig. 5 together with ionization distances calculated using hydrogenic theory for the most strongly surface oriented $m=0$, $n_1=0$ Stark states [6]. The calculated values increase as $3.4n^2$, i.e., as the geometrical size of the atom, consistent with the n^2 scaling observed in earlier studies of ionization thresholds. The good agreement between theory and experiment is encouraging.

The present work demonstrates that charge transfer during atom-surface collisions is strongly influenced by surface-induced perturbations in the energies and structure of the atomic states. Rydberg atoms provide a powerful probe of such effects and into the behavior of atoms near surfaces in general. Although this work focused on thick gold samples, studies with very thin (1–10 nm) conducting films grown epitaxially on insulating substrates are also of interest. Calculations suggest that for such films quantum size effects become important and can strongly influence tunneling rates [18,19].

It is a pleasure to acknowledge valuable discussions with Professor H. Winter (Berlin). This research was supported by the National Science Foundation under Grant No. PHY0353424 and by the Robert A. Welch Foundation. S.W. also acknowledges support from Professor H. Winter and the Deutsche Forschungsgemeinschaft (DFG Grant No. Wi1336) during his time at Rice. J.C.L. received support from the Naval Research Laboratory.

[1] A. V. Chaplik, Zh. Eksp. Teor. Fiz. **54**, 332 (1968) [Sov. Phys. JETP **27**, 178 (1968)].
[2] P. Nordlander, Phys. Rev. B **53**, 4125 (1996).
[3] P. Nordlander and F. B. Dunning, Phys. Rev. B **53**, 8083 (1996).
[4] P. Nordlander and F. B. Dunning, Nucl. Instrum. Methods Phys. Res. B **125**, 300 (1997).
[5] P. Kürpick, U. Thumm, and U. Wille, Phys. Rev. A **57**, 1920 (1998).
[6] N. N. Nedeljkovic and Lj. D. Nedeljkovic, Phys. Rev. A **72**, 032901 (2005).
[7] J. Braun and P. Nordlander, Surf. Sci. **448**, L193 (2000).
[8] C. Oubre, P. Nordlander, and F. B. Dunning, J. Phys. Chem. B **106**, 8338 (2002).
[9] Z. Zhou, C. Oubre, S. B. Hill, P. Nordlander, and F. B. Dunning, Nucl. Instrum. Methods Phys. Res. B **193**, 403 (2002).
[10] F. B. Dunning, H. R. Dunham, C. Oubre, and P. Nordlander, Nucl. Instrum. Methods Phys. Res. B **203**, 69 (2003).
[11] C. Fabre, M. Gross, J. M. Raimond, and S. Haroche, J. Phys. B **16**, L671 (1983).
[12] C. A. Kocher and C. R. Taylor, Phys. Lett. A **124**, 68 (1987).
[13] D. F. Gray, Z. Zheng, K. A. Smith, and F. B. Dunning, Phys. Rev. A **38**, 1601 (1988).
[14] J. M. McGuirk, D. M. Harber, J. M. Obrecht, and E. A. Cornell, Phys. Rev. A **69**, 062905 (2004).
[15] S. B. Hill, C. B. Haich, Z. Zhou, P. Nordlander, and F. B. Dunning, Phys. Rev. Lett. **85**, 5444 (2000).
[16] S. B. Hill, C. A. Haich, F. B. Dunning, G. K. Walters, J. J. McClelland, R. J. Celotta, and H. G. Craighead, Appl. Phys. Lett. **74**, 2239 (1999).
[17] R. F. Stebbings, C. J. Latimer, W. P. West, F. B. Dunning, and T. B. Cook, Phys. Rev. A **12**, 1453 (1975).
[18] B. Bahrim, P. Kürpick, U. Thumm, and U. Wille, Nucl. Instrum. Methods Phys. Res. B **164–165**, 614 (2000).
[19] U. Thumm, P. Kürpick, and U. Wille, Phys. Rev. B **61**, 3067 (2000).